processes

MDPI

Article

Flow Performance Analysis of Double-Chamber Gas–Liquid Transferring Device

Si Huang [1,*], Yantao Hu [1], Tianri Guan [2], Hao Fu [2] and Ziqiang Pan [2]

[1] School of Mechanical and Automotive Engineering, South China University of Technology, Guangzhou 510641, China; 202120101659@mail.scut.edu.cn
[2] GuanFu Energy Technology Co., Ltd., Guangzhou 510555, China
* Correspondence: huangsi@scut.edu.cn; Tel.: +86-13725200827

Abstract: Gas–liquid transportation is an efficient and economical transportation technology developed in recent years. It mainly uses some transportation equipment to simultaneously transport crude oil, associated natural gas, produced water, and so on for the purpose of reducing costs and energy consumption. In this paper, a double-chamber gas–liquid transferring device was selected as the research object. The VOF multiphase flow model of FLUENT software was used to simulate the gas–liquid two-phase flow performance under the design condition. The relationships between the two-phase flows, pressure, temperature, liquid level in the tank, outlet flow rate of the device, and time were calculated and analyzed. The results show that the operating cycle of the device can be divided into three processes, namely 'suction-compression-discharge', in which the cycle period formula is proposed as well. The pressures of gas and liquid in the device are basically the same, but the temperatures of the two phases are quite different in the compression process. In the compression process, the outlet valve is closed so that the outlet flow rate of the device is zero, and the gas compression process can be approximately treated as isothermal compression in engineering design. The comparison between the measured performance data in the oil field and the calculation results indicates that the calculation method in this paper is feasible for the performance prediction and optimization of the double-chamber gas–liquid transferring device.

Keywords: double-chamber; gas–liquid transportation; flow performance; operating cycle

Citation: Huang, S.; Hu, Y.; Guan, T.; Fu, H.; Pan, Z. Flow Performance Analysis of Double-Chamber Gas–Liquid Transferring Device. *Processes* **2023**, *11*, 1311. https://doi.org/10.3390/pr11051311

Academic Editors: Basma Souayeh, Fateh Mebarek-Oudina, Wael Al-Kouz and Udo Fritsching

Received: 14 March 2023
Revised: 3 April 2023
Accepted: 22 April 2023
Published: 24 April 2023

1. Introduction

With the continuous development of oil production and transportation, it is important to achieve energy conservation and reduce emissions, production costs, and environmental pollution. In the process of oilfield exploitation, crude oil, associated natural gas, and underground water are usually produced from oil wells at the same time, so it is possible to gain economic benefits from oilfield development using a pipeline to transfer liquids (oil, water) together with gas (natural gas). The key equipment in gas–liquid transportation is the gas–liquid pump. At present, there are two main types of gas–liquid pumps widely applied in oil fields, i.e., twin-screw pumps and rotodynamic pumps. For twin-screw pumps, the world's first twin-screw pump was invented in 1890. In the following decades, various kinds of screw pumps were developed for engineering applications, especially for oil-gas transportation [1–3]. Vetter and Wincek [4] proposed an analytical model to predict the volumetric flow capacity for both single-phase and two-phase operations of twin-screw pumps. Egashira et al. [5] conducted a qualitative study on the relationship between leakage and factors such as the gas content of the screw pump, the rotor speed, and the pressure difference between the inlet and outlet. They also provided an empirical model for calculating the internal pressure distribution of the oil-gas twin-screw pump. Muhammed [6] developed a model for predicting the dynamic pressure field around the screws and the dynamic response of twin-screw pump rotors due to hydrodynamic forces.

Sun et al. [7] investigated the two-phase flow mechanism inside a double suction twin-screw pump under different inlet gas volume fractions (GVF). Their results showed that the pressure inside the working chamber was symmetrical and increased gradually from the inlet to the outlet. The high GVF areas on the surface of the rotors mainly existed at the positions of gaps.

For rotodynamic pumps, the earliest research on multiphase rotodynamic pumps began in the 1980s and was put into engineering application in the 1990s [8–11]. Huang et al. [12,13] conducted a three-dimensional numerical simulation of gas–liquid two-phase flows in a helico-axial pump, and provided a numerical method for the performance prediction of the pump. Ma et al. [14] carried out a multi-objective optimization design for rotodynamic pumps. The relative head and efficiency of the multiphase pump were increased by 0.81% and 0.77%, respectively. Suh et al. [15] also performed a numerical optimization to enhance the hydraulic performance of a helico-axial multiphase pump. The single-objective (efficiency) optimization was conducted for both the impeller and diffuser. The objective function was evaluated at design points using Latin-hypercube sampling. Their results showed remarkable increases in a higher performance level compared with the base model. Liu et al. [16] proposed a method to optimize the performance of multi-stage multiphase pumps by theoretical analysis based on the Oseen vortex, and the pump head and efficiency could be improved by an average of 0.29% and 0.19%, respectively. In summary, a lot of work was reported on the design and performance analysis of twin-screw and rotodynamic pumps for gas–liquid transportation.

In addition, Guan et al. [17,18] recently developed a novel double-chamber gas–liquid transferring device. In this device, two tanks alternately become the suction chamber and the compression-discharge chamber for the incoming gas–liquid flows. A liquid pump is used to transfer liquids from one tank to the other, thereby realizing the continuous transportation of the gas–liquid medium. The device was already applied in oilfields and is expected to become an effective gas–liquid two-phase transferring tool with wide application prospects, due to its simple structure and adaptability to various inflow conditions. However, the working principles and operating cycle laws in this kind of double-chamber gas–liquid transferring device are still unclear. In this paper, therefore, the gas–liquid two-phase flows field in a double-chamber gas–liquid transferring device was simulated numerically using FLUENT software, to understand the working principle of the device and the internal mechanism of gas–liquid two-phase flows, and to provide a theoretical basis for improving the design of the double-chamber gas–liquid transferring device.

2. Working Principle and On-Site Performance Measurement

The double-chamber gas–liquid transferring device (Figure 1) is mainly composed of three major systems, i.e., a fluid system (liquid pump, circulating tanks and pipeline, etc.), a control system (reversing valves, one-way valves and intelligent control system, etc.), and an instrument air system (air compressor, pipeline, etc.). The geometric parameters of the tanks and pipes are shown in Table 1.

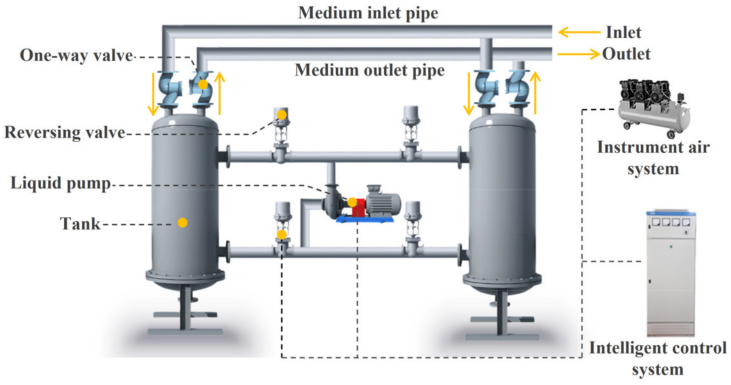

Figure 1. Double-chamber Gas–liquid Transferring Device.

Table 1. Major dimension parameters in device.

Component	Specification (mm)
Circulation tank	DN = 800, S = 8, H = 1950
Suction and discharge pipe	Φ159 × 6
Inlet pipe for liquid pump	Φ159 × 6
Outlet pipe for liquid pump	Φ133 × 6

During the operation of the device, when liquid is transferred from tank 1 to tank 2 using the liquid pump, tank 1 and tank 2 are the suction chamber and compression-discharge chamber for the inflow medium, respectively. As shown in Figure 2a, the reversing valves 2# and 3# are open, while valves 1# and 4# are closed. The incoming gas–liquid mixture flows through the inlet pipeline into tank 1, guided by the one-way valve. The gas–liquid mixture is separated in tank 1 due to gravity, and the liquid in the bottom is pumped and pressurized by the liquid pump to tank 2. The liquid level in tank 1 decreases and the liquid level in tank 2 increases. When the liquid level in tank 2 is high enough to make the pressure in the tank reach the set superior limit, the intelligent control system will open the outlet valve of the device, and the gas–liquid medium in tank 2 will be discharged from the outlet of the device. When the liquid level in tank 1 drops to the set lower limit (25% liquid level), the reversing valves are automatically switched by the intelligent control system. Reversing valves 1# and 4# are open, 2# and 3# are closed, and the device outlet is temporarily closed. At this moment, tank 1 and tank 2 exchange functions. The incoming medium flows into tank 2, guided by the one-way valve, and the gas–liquid separation is carried out in tank 2. The liquid is pressurized by the liquid pump from tank 2 to tank 1, and the medium in tank 1 flows out from the outlet pipe after the pressure reaches the set value (Figure 2b). In this way, the continuous pumping and transportation of the gas–liquid mixture is ultimately achieved.

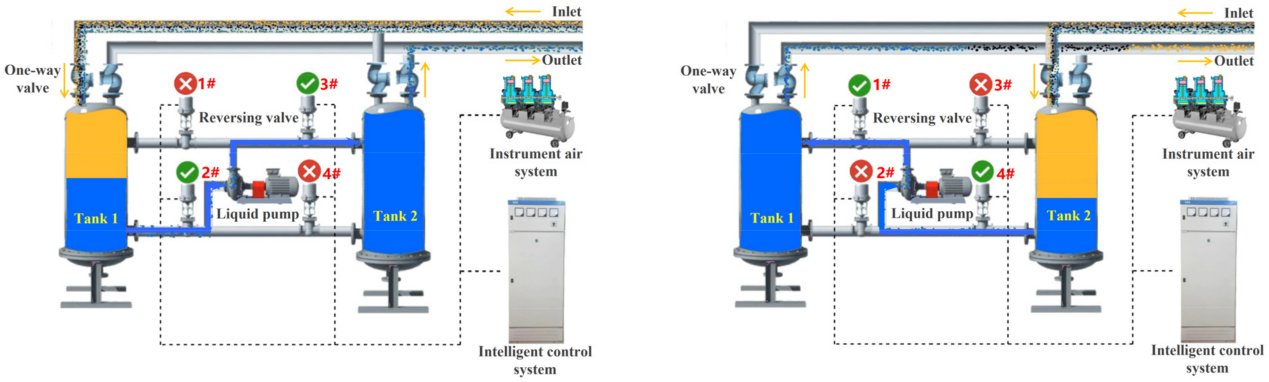

Figure 2. Working Principle of Double-chamber Gas–liquid Transferring Device: (**a**) Tank 1 as Suction Chamber; (**b**) Tank 2 as Suction Chamber.

The operating conditions of the device in an oil field were as follows: the pressure of the inflow medium p_s = 0.28 MPa and the gas volume fraction α = 20%, the outlet pressure p_d = 0.83 MPa, liquid pump flow Q_{by} = 16 L/s. Table 2 shows the average values of the on-site measured pressure difference between the inlet and outlet, flow rates, and valve switching time. In the table, the gas flow rates are converted to those at the standard condition.

Table 2. Comparison of measured and calculated results of gas–liquid transferring device.

	Switching Time (s)	Gas (m^3/h)	Liquid (m^3/h)	Pressure Difference between Inlet and Outlet (MPa)
On-site measurement	177	38.53	57.38	0.54
Simulation	172.53	37.23	57.6	0.55
Relative error	2.53%	3.37%	3.83%	1.85%

3. Numerical Method

According to the data on the tank and pipes shown in Table 1, the 3D fluid computational domain of the double-chamber gas–liquid transferring device was created using the CAD software SolidWorks as shown in Figure 3.

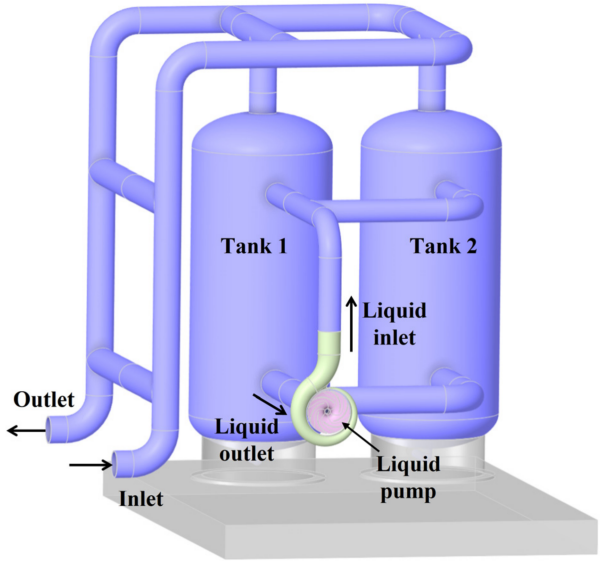

Figure 3. Flow Computational Domain of Device.

The independence verification for the computational grid was performed as shown in Figure 4. The time interval that the outlet pressure of the device reached the set value from the initial state was taken as the indicator for investigation. The polyhedral grids with different grid densities were selected for calculation because the number of polyhedral meshes could be much less than that of tetrahedral meshes with the same accuracy. Since the numerical simulations were made for the whole model of the device and a short time step was required for the two-phase flow in the study, it took more than three weeks to calculate a complete working cycle using a Dell Workstation (Precision Tower 7920). Based on the results in Figure 4, the polyhedron grid with grid number 392860 and node number 2102518 was finally selected as the computational do-main grid for the subsequent calculation, considering both calculation cost and accuracy.

The VOF multiphase model [19] and the RNG$k-\varepsilon$ turbulence model [20] in FLUENT software were selected to simulate the three-dimensional gas–liquid two-phase flow field in the device. Air was treated as an ideal gas (compressible) and the primary phase, and water was the liquid phase (incompressible) as the secondary phase. The phase change was neglected, but the energy equation was solved with consideration of heat transfer. The direction of gravity (9.81 m/s^2) was set according to the actual situation. The ambient conditions were the atmospheric pressure (101,325 Pa) and 15 °C in temperature.

In terms of the boundary conditions of the computational domain, the inlet of the device was set as the pressure inlet, and the temperature of the inflow medium was 48 °C. The outlet of the device was set as a pressure outlet as well. To simplify the calculation, the 3D flow field inside the liquid pump was not simulated. However, the effect of the

liquid pump was applied by setting the boundary conditions (flow rates of the pump) at the pipes connected to the pump. The check valve and the directional valve group were set to the 'wall' or the 'internal surface' according to the operational orders. When the liquid level in the tank was lowered to about 25%, the TUI command in the software was executed through the Execute Commands function [21] to realize the switching between the suction chamber and the compression-discharge chamber. The PISO algorithm was used in the solver, the second-order upwind discretization scheme was used for the continuity equation and momentum equations, the Geo-Reconstruct scheme was used for the phase volume fraction, the first-order implicit scheme was used for the time discretization, and the calculation time step was $\Delta t = 0.001$ s.

Table 2 gives the comparison between the on-site performance measurement and the calculation results, in order to verify the validity of the calculation method. It can be seen from Table 2 that the errors between the calculated and the measured data are within a reasonable range, indicating the calculation method and results in this study are feasible.

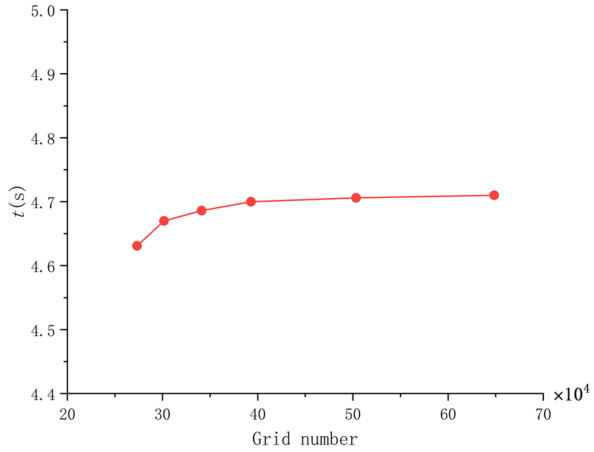

Figure 4. Grid Independence Test.

4. Result Analysis

4.1. Liquid Level and Gas–Liquid Two-Phase Distribution

Figure 5 shows the calculated distribution of gas volume fraction at different liquid levels. The initial state of the calculation was that the two tanks were filled with liquid and the pipeline was filled with gas (Figure 5a). After the device started to operate, the gas–liquid medium entered the device from the inlet in the design condition. The gas–liquid separation was formed in tank 1 due to gravity (Figure 5b), and the inflow of the liquid pump was not entrained with gas phase content. The liquid level in tank 1 was further lowered as the liquid in tank 1 was continuously transported to tank 2 (Figure 5c). When the liquid level in tank 1 dropped to the set lower limit, the reversing valves automatically switched. After switching, the gas–liquid medium entered tank 2 from the inlet of the device and formed phase separation. As the liquid in tank 2 was pressurized by the pump into tank 1, the gas–liquid medium in tank 1 was compressed and discharged out of the outlet of the device (Figure 5d–f).

Figure 6 shows the variation of relative liquid level H^* with time in two tanks. The relative liquid level H^* is defined as:

$$H^* = H_l / H \tag{1}$$

where H_l is the liquid level in the tank, H is the total height of the tank.

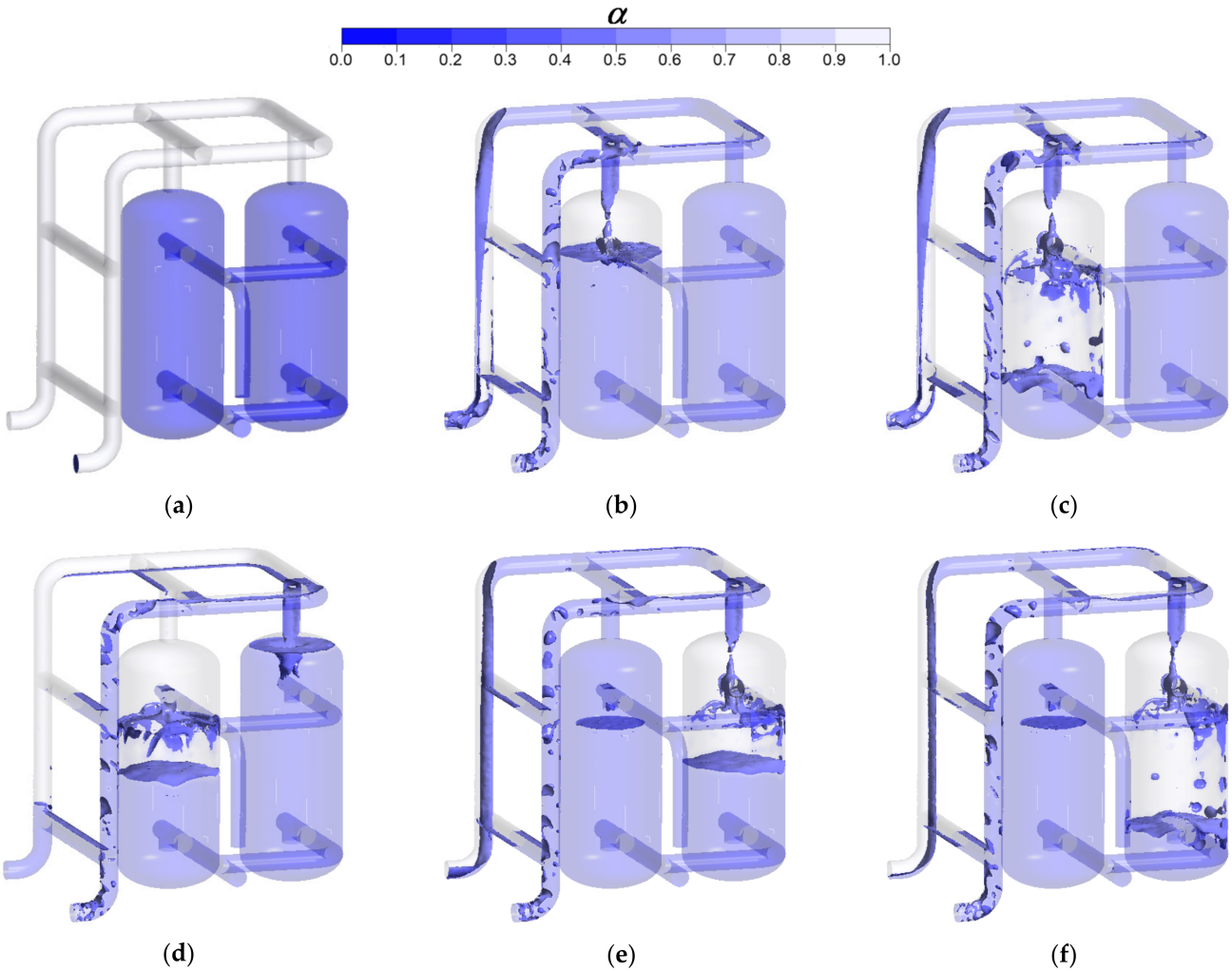

Figure 5. Gas Volume Fraction α Distribution in the Device under Different Liquid Levels: (**a**) Initial state; (**b**) Liquid Level Dropped to 75% in Tank 1; (**c**) Liquid Level Dropped to 25% in Tank 1; (**d**) Liquid Level Rose to 50% in Tank 1; (**e**) Liquid Level Dropped to 50% in Tank 2; (**f**) Liquid Level Dropped to 25% in Tank 2.

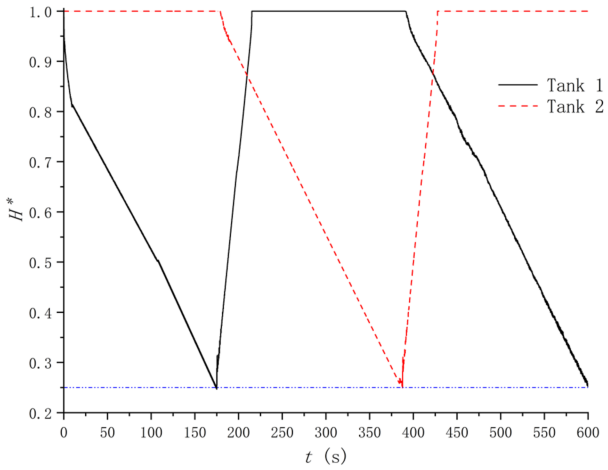

Figure 6. Variation of Liquid Level in Two Tanks with Time.

From Figure 6, it can be seen the liquid levels in the two tanks rise and drop periodically and alternately. The cycles of liquid level drop and rise are T_1 and T_2, which can be calculated by Equations (2) and (3), respectively.

$$T_1 = V_e/\alpha Q_{\mathrm{by}} \tag{2}$$

$$T_2 = V_e/Q_{\mathrm{by}} \tag{3}$$

where V_e is the effective filling space of the tank to remove the lowest liquid level.

It can be seen from the Equations (2) and (3) that the period of liquid level drop or rise is related to the inlet gas content α, liquid pump flow Q_{by}, and the size of the circulating tank.

Some features are also found in Figure 6 as follows. At the beginning, the liquid level in tank 1 continued to decline as the liquid was pumped from tank 1 to tank 2, and the liquid level in tank 2 remained full. However, the liquid in tank 1 was supplemented to some degree from the inflow, so the liquid level dropped slowly with a decreasing speed to a value of about $H^* = 0.25$. At this time, the reversing valves automatically switched. The liquid in tank 2 was delivered to tank 1 by the pump, which made tank 1 full of liquid in a relatively short time. When the liquid level in tank 2 gradually decreased to a value of about $H^* = 0.25$, the reversing valve switched again into the next operating cycle.

4.2. Pressure, Temperature, and Flow Rate

Figure 7 shows the calculated average pressure of the gas–liquid two-phase medium in the tank with time. It can be seen from Figure 7 that the pressures in both the gas phase and the liquid phase were basically the same. When the device started working, the valve of tank 2 was closed until the pressure in tank 2 rose to the set value (0.83 MPa). The pressure in tank 1 increased slightly but was basically consistent with the inlet pressure of the device (0.28 MPa). This process was regarded as the 'suction process' (for tank 1, the same below). With the switching of the valve, the pressure in tank 2 decreased sharply due to the opening of the inlet valve and the closing of the outlet valve of tank 1, and the boosting effect of the liquid pump continuously increased the pressure in tank 1 to the set value, which was the 'compression process'. When the pressure in tank 1 reached the set value, the valve opened, and the gas–liquid medium in tank 1 maintained the set pressure to discharge from the outlet of the device. This process was the 'discharge process'. So far, tank 1 completed an operating cycle, which included three processes of 'suction-compression-discharge'. Comparing Figures 6 and 7, it can be found that the cycle period T of the device is the sum of the liquid level drop times of tank 1 and tank 2. The suction time is equal to the liquid level drop time of tank 1, and the sum of the compression and the discharge time is equal to the liquid level drop time of tank 2. Tank 1 and tank 2 are usually the same size, so an operating cycle period T is:

$$T = 2T_1 = 2V_e/\alpha Q_{by} \tag{4}$$

Figure 8 shows the calculated pressure distribution in the device during an operating cycle. In the suction process (Figure 8a), the pressure in tank 1 was basically consistent with the inlet pressure of the device, while the pressure in tank 2 was consistent with the outlet pressure of the device. In the compression process (Figure 8b), however, the pressure in tank 1 gradually increased but not yet reached the set value. The pressure in tank 2 was consistent with the inlet pressure of the device. In the discharge process (Figure 8c), the pressure in tank 1 reached the set value and was consistent with the outlet pressure of the device, and the pressure in tank 2 was consistent with the inlet pressure of the device.

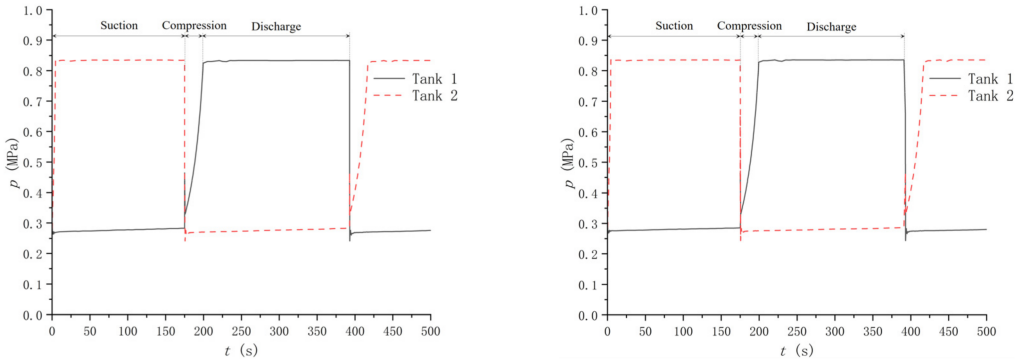

Figure 7. Average Pressure in Tanks with Time: (**a**) Gas Phase; (**b**) Liquid Phase.

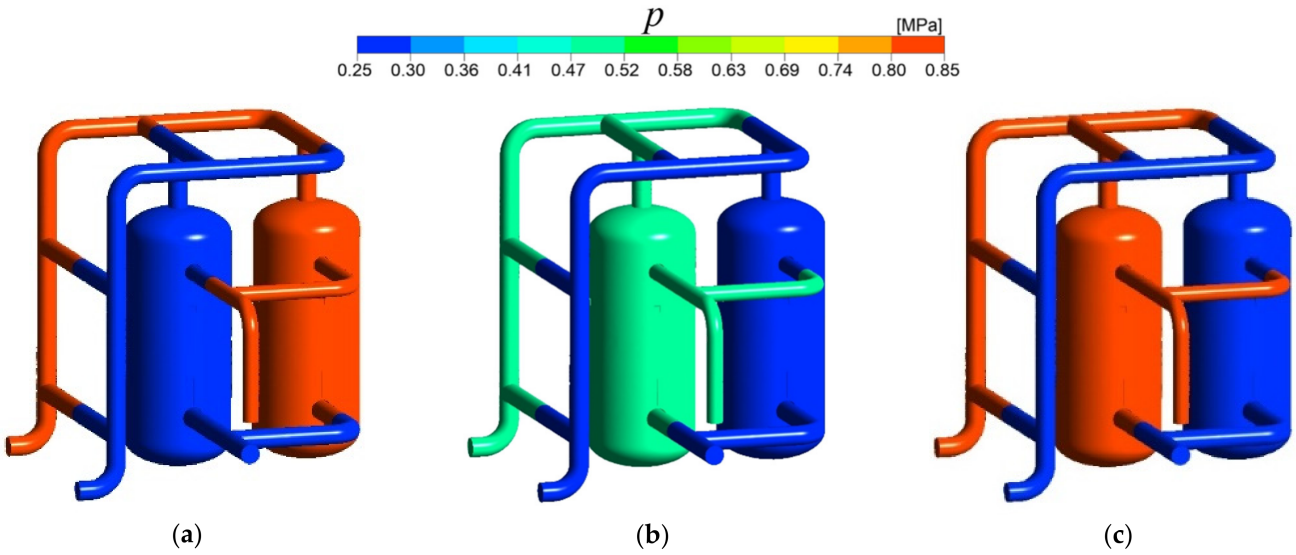

Figure 8. Pressure Distribution in the Device during an Operating Cycle: (**a**) Suction Process; (**b**) Compression Process; (**c**) Discharge Process.

Figure 9 shows the calculated average temperature of the two-phase medium in the tanks with time. It can be seen from Figure 9 that the temperatures in both the gas and the liquid were basically the same in the suction and discharge processes, and maintained at about 48 °C. In the compression process, however, the gas temperature rose considerably due to the compression by the liquid, and the maximum temperature difference with the inlet was about 23 °C. Meanwhile, the liquid temperature also rose due to heat exchange between the two phases, but the maximum temperature difference with the inlet was about 6 °C.

Figure 10 shows the calculated temperature distribution in the device during an operating cycle. It can be seen from Figure 10 that the temperature in the device was maintained at about 48 °C in the suction process and the discharge process. In the compression process, the temperature distribution was quite different because the gas was compressed to increase the temperature and exchange heat with the liquid. High temperatures mainly occurred in the upper part of the tank and in the area with more gas.

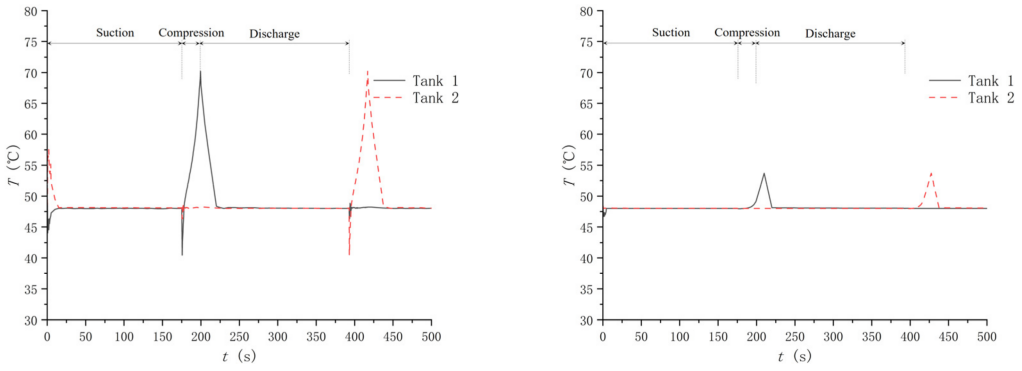

Figure 9. Average Temperature in Tanks with Time: (**a**) Gas Phase; (**b**) Liquid Phase.

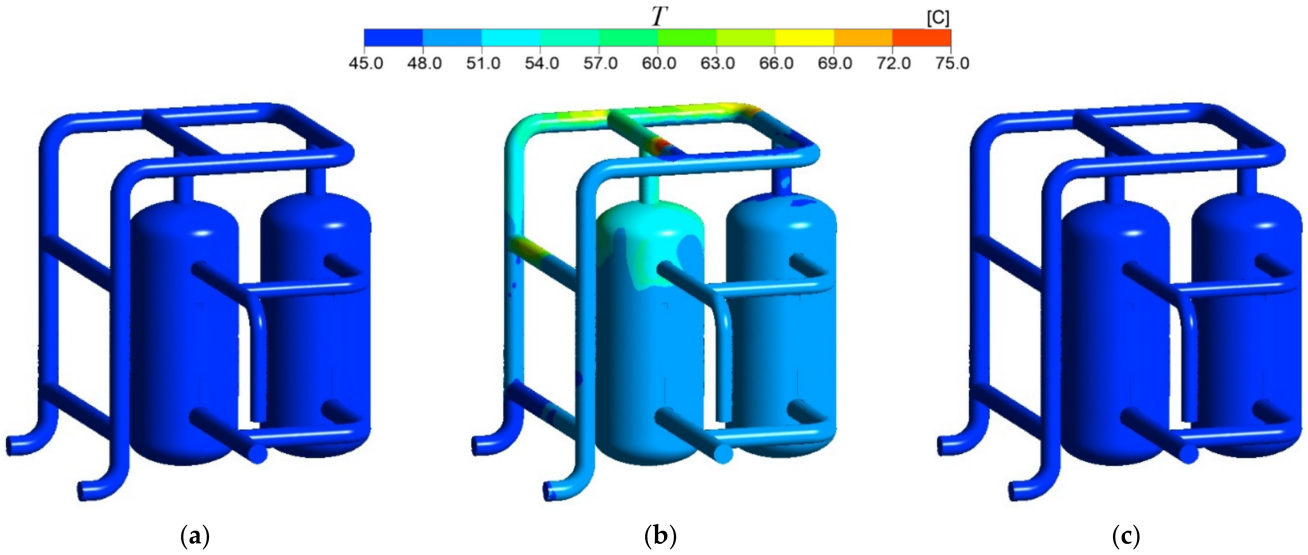

Figure 10. Temperature Distribution in the Device during an Operating Cycle: (**a**) Suction Process; (**b**) Compression Process; (**c**) Discharge Process.

Figure 11 shows the calculated outlet flow of the device with time. It can be seen from Figure 11 that the outlet flow of the device fluctuates around Q_p = 17.3 L/s in the suction process and the discharge stage. In the compression process, however, the outlet valve of the device was closed until the pressure in the tank rose to the set value (0.83 MPa), so the outlet flow of the device in the compression process was $Q_p = 0$.

In order to understand the general law of the gas compression process of the device, Figure 12 shows the relationship between the calculated average pressure p and the average density ρ of the gas in tank 1 during the compression process, together with the theoretical curves of the isothermal process and adiabatic process of an ideal gas [22]. It can be seen from Figure 12 that the $p - \rho$ curve during the gas compression process in the tank quite meets that of the isothermal process, due to the absorption and the removal of the heat by the operating liquid. In engineering design, therefore, the gas compression process in the device can be approximately regarded as an isothermal process similar to the treatment of gas in liquid ring compressors [23,24].

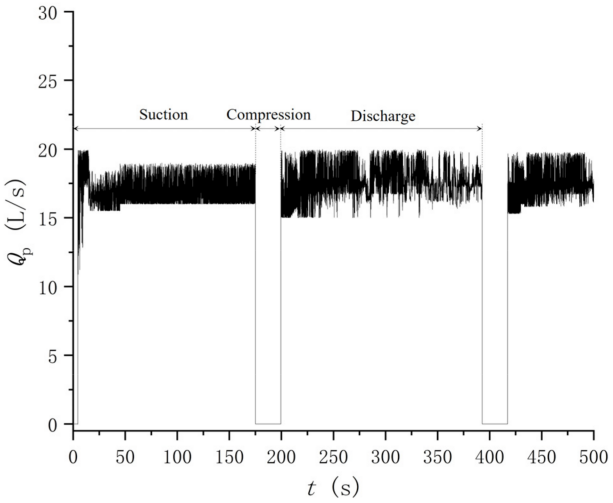

Figure 11. Outlet Flow Rate of the Device with Time.

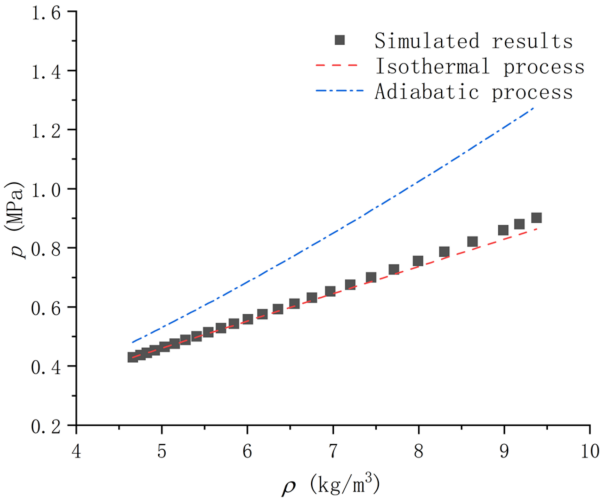

Figure 12. Gas Compression Process in Tank.

5. Conclusions

In this work, through the transient two-phase flow numerical simulation of the double-chamber gas–liquid transferring device, the following conclusions are obtained:

- During the operation of the device, the gas–liquid medium forms phase separation in the circulating tanks due to gravity, and the inflow of the liquid pump is not entrained with the gas phase content. The liquid levels in the two tanks rise and drop periodically and alternately. The period of liquid level drop or rise is related to the inlet gas content α, liquid pump flow Q_{by} and the volume of the circulating tank, which can be calculated by Equations (2) and (3), respectively.
- The operating cycle of the device can be divided into three processes, 'suction-compression-discharge', and the cycle period can be calculated according to Equation (4). The pressure in the tank in the suction chamber is basically consistent with the inlet pressure of the device, and the pressure in the tank in the discharge chamber is basically consistent with the outlet of the device. In the compression process, there is no outlet flow because the outlet valve of the device is temporarily closed, and the circulating tank as the discharge chamber is in a compressed state.
- In the suction and discharge processes, the temperatures of both phases in the device are basically the same, but there are significant differences in the compression process. Due to the absorption and the removal of the heat by liquid, the relationship between

gas pressure and gas density is close to the isothermal compression process for an ideal gas, so the compression process of the gas phase in the tanks can be approximately treated as an isothermal process in engineering design.

- The double-chamber gas–liquid transferring devices are expected to become an effective gas–liquid two-phase transferring tool with wide application prospects, due to their simple structure and adaptability to various inflow conditions. For the next study, the influence of various factors on the flow performance will be analyzed, including operating conditions (inlet gas content, liquid pump flow, etc.) and structural parameters (pipeline, circulation tank, etc.).

Author Contributions: Conceptualization, S.H., T.G. and H.F.; methodology, S.H. and Y.H.; software, S.H. and Y.H.; validation, S.H., Y.H. and Z.P.; formal analysis, S.H. and Y.H.; investigation, S.H.; resources, S.H. and T.G.; data curation, S.H. and Y.H.; writing—original draft preparation, S.H. and Y.H.; writing—review and editing, S.H. and Y.H.; visualization, Y.H.; supervision, S.H. and T.G.; project administration, S.H. and T.G.; funding acquisition, S.H. and Z.P. All authors have read and agreed to the published version of the manuscript.

Funding: This research received no external funding.

Data Availability Statement: The data presented in this study are available on request from the corresponding author.

Conflicts of Interest: The authors declare no conflict of interest.

References

1. Mobbs, A. Subsea Multiphase Pumps in the Zafiro/Topacio Project. In Proceedings of the 4th Annual Texas A&M Multiphase Pump User Roundtable (MPUR), Houston, TX, USA, 9 May 2002.
2. Saadawi, H.; Al Olama, S. Application of Multiphase Pumps in a Remote Oil Field Onshore Abu Dhabi. In Proceedings of the Middle East Oil Show Conference, Sakhir, Bahrain, 9–12 June 2003.
3. Martin, A.M. Multiphase Twin-Screw Pump Modeling for the Oil and Gas Industry. Ph.D. Thesis, Texas A&M University, College Station, TX, USA, 2003.
4. Vetter, G.; Wincek, M. Performance prediction of twin-screw pumps for two-phase gas/liquid flow. *ASME* **1993**, *154*, 331–340.
5. Egashira, K.; Shoda, S.; Tochikawa, T.; Furukawa, A. Backflow in twin-screw-type multiphase pump. *SPE Prod. Facil.* **1998**, *13*, 64–69. [CrossRef]
6. Muhammed, A.R.A.H. Rotordynamics of Twin-Screw Pumps. Ph.D. Thesis, Texas A&M University, College Station, TX, USA, 2013.
7. Sun, S.H.; Wu, P.B.; Guo, P.C.; Yi, G.Z.; Kovacevic, A.; Zhang, H.; Wu, G.K. Numerical investigation on a double suction twin-screw multiphase pump. *IOP Conf. Series Earth Environ. Sci.* **2021**, *774*, 12048. [CrossRef]
8. Skiftesvik, P.K.; Svaeren, J.A. Muliphase Pumps and Flow Meters-Status of Field Testing. In Proceedings of the Offshore Technology Conference, Houston, TX, USA, 1–4 May 1995.
9. Engelam, E.; Torp, A.T. The Poseidon project and the future of multiphase production. In Proceedings of the Offshore Northern Seas Conference, Stavanger, Norway, 28–31 August 1990.
10. Tosta Da Silva, L.; Carbone, L.C.; Coelho, E.J.D.J.; Cerqueira, M.B.; Kuchpil, C.; Maia De Souza, C.E. Barracuda Subsea Helico-Axial Multiphase Pump Project. In Proceedings of the MSOTC Conference, Houston, TX, USA, 6–9 May 2013.
11. Anwar, Z.; Electric, G. Subsea Technology Multiphase Pumping. In Proceedings of the SPE/IATMI Asia Pacific Oil & Gas Conference and Exhibition, Jakarta, Indonesia, 17 October 2017.
12. Huang, S.; Xue, D. Calculation of the internal flow in helico-axial type gas-liquid two-phase pump. In Proceedings of the International Conference on Pumps and Fans, Beijing, China, 1 January 1998.
13. Huang, S.; Xue, D. Three-dimensional calculation of gas-oil two-phase flow in helico-axial booster-pump impeller. In Proceedings of the 1st International Conference on Engineering Thermophysics, Beijing, China, 1 January 1999.
14. Ma, X.; Li, X.; Yang, D. Multi-objective Optimization design of the multiphase pump boosting cell. In Proceedings of the 2011 Second International Conference on Mechanic Automation and Control Engineering, Inner Mongolia, China, 15 July 2011.
15. Suh, J.; Kim, J.; Choi, Y.; Joo, W.; Lee, K. A study on numerical optimization and performance verification of multiphase pump for offshore plant. *Proc. Inst. Mech. Eng. Part A J. Power Energy* **2017**, *231*, 382–397. [CrossRef]
16. Liu, M.; Tan, L.; Xu, Y.; Cao, S. Optimization design method of multi-stage multiphase pump based on Oseen vortex. *J. Pet. Sci. Eng.* **2020**, *184*, 106532. [CrossRef]
17. Guan, T. Dual-Chamber Liquid Reciprocating Multiphase Flow Mixing Method and Device. U.S. Patent CN201811286148.0, 1 January 2019.

18. GuanFu Science and Technology Energy Co., Ltd. Application Case of GuanFu Mixed Transport Device. 2022. Available online: http://www.guanfukeji.com/PicList.aspx?ClassID=27 (accessed on 30 June 2022).
19. Hirt, C.W.; Nichols, B.D. Volume of fluid (VOF) method for the dynamics of free boundaries. *J. Comput. Phys.* **1981**, *39*, 201–225. [CrossRef]
20. Yakhot, V.; Orszag, S.A. Renormalization group analysis of turbulence. I. Basic theory. *J. Sci. Comput.* **1986**, *1*, 3–51. [CrossRef]
21. Ansys Inc. *ANSYS Fluent Users Guide*; Release 2021 R1; Ansys Inc.: Canonsburg, MI, USA, 2021.
22. Yunus, A.C.; Michael, A.B. *Thermodynamics: An Engineering Approach*, 8th ed.; McGraw-Hill: New York, NY, USA, 2015.
23. Faragallah, W.H. *Liquid Ring Vacuum Pumps and Compressors*; Gulf: Houston, TX, USA, 1988.
24. Bannwarth, H. *Liquid Ring Vacuum Pumps, Compressors and Systems: Conventional and Hermetic Design*; John Wiley & Sons: Hoboken, TX, USA, 2006.